10.1098/rsta.2003.1214

THE ROYAL SOCIETY

Nanoscale solid-state quantum computing

By A. Ardavan[1], M. Austwick[2], S. C. Benjamin[2], G. A. D. Briggs[2], T. J. S. Dennis[3], A. Ferguson[4], D. G. Hasko[4], M. Kanai[3], A. N. Khlobystov[2], B. W. Lovett[2], G. W. Morley[1], R. A. Oliver[2], D. G. Pettifor[2], K. Porfyrakis[2], J. H. Reina[1], J. H. Rice[1], J. D. Smith[1], R. A. Taylor[1], D. A. Williams[5], C. Adelmann[6], H. Mariette[6] and R. J. Hamers[7]

[1]*Clarendon Laboratory, Parks Road, Oxford OX1 3PU, UK*
[2]*Department of Materials, University of Oxford, Parks Road, Oxford OX1 3PH, UK*
[3]*Department of Chemistry, Queen Mary, University of London, Mile End Road, London E1 4NS, UK*
[4]*Cavendish Laboratory,* [5]*Hitachi Cambridge Laboratory, Madingley Road, Cambridge CB3 0HE, UK*
[6]*CEA Grenoble, 17 Rue des Martyrs, 38054 Grenoble Cedex 9, France*
[7]*Department of Chemistry, University of Wisconsin, Madison, WI 53706, USA*

Published online 11 June 2003

Most experts agree that it is too early to say how quantum computers will eventually be built, and several nanoscale solid-state schemes are being implemented in a range of materials. Nanofabricated quantum dots can be made in designer configurations, with established technology for controlling interactions and for reading out results. Epitaxial quantum dots can be grown in vertical arrays in semiconductors, and ultrafast optical techniques are available for controlling and measuring their excitations. Single-walled carbon nanotubes can be used for molecular self-assembly of endohedral fullerenes, which can embody quantum information in the electron spin. The challenges of individual addressing in such tiny structures could rapidly become intractable with increasing numbers of qubits, but these schemes are amenable to global addressing methods for computation.

Keywords: quantum computing; nanomaterials; quantum dots; nanotubes; endohedral fullerenes; global addressing

1. Introduction

In some ways the present effort to build a quantum computer is analogous to attempts to build an aeroplane 100 years ago: not everyone was convinced that it would be possible, but there were enough people who were sufficiently enthusiastic and sufficiently determined that eventually success did come along. It came in more than one form, and early powered flights were made independently in Europe and in America.

One contribution of 20 to a Discussion Meeting 'Practical realizations of quantum information processing'.

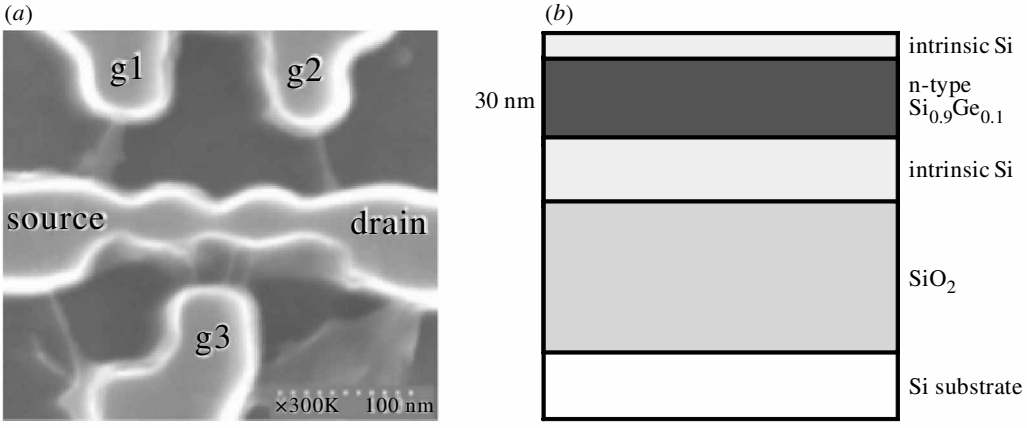

Figure 1. Scanning electron micrograph of a SiGe double QD. The dark areas around the structure are where material has been removed by reactive ion etching. The diameter of each dot is *ca.* 40 nm.

Different aeroplanes had different designs. A key issue was control: early gliders used a shift of body weight; the first powered flights used wing warping; a few years later the now ubiquitous aileron was introduced. Other changes came much later: the jet engine of a modern airliner works on quite different principles from the piston driven propellers of the first half of the 20th century.

The ability to understand and control materials on the nanoscale opens up a range of possibilities for making devices in which quantum effects dominate. Some of these may prove useful for classical information processing, perhaps because they can be made sufficiently small that they leapfrog the challenges facing future progress in miniaturization and complexity. Others may be useful for quantum computing, which offers the possibility to solve certain problems that could not realistically be tackled by classical information processing. None of the various possibilities has yet been made into a working quantum computer. Several solid-state approaches are being pursued, with the passion and conviction that are a necessary (though not sufficient) condition for success.

2. Nanofabricated devices

Although the size of devices that can be mass produced is limited by ultraviolet lithography, much smaller devices can be made using electron beam lithography (EBL). In this way, designer structures can be made with line widths as small as 4 nm (Yasin *et al.* 2001). This degree of control permits quantum dots (QDs) to be fabricated in which the effect of adding a single electron becomes significant, and where the separation between dots can be controlled so that quantum mechanical interactions are also significant. In this way it is possible to independently control the number of electrons on each dot. Coupled with a read-out electrometer, this, in itself, provides a single-electron memory for classical information (Stone & Ahmed 1998). The challenge for the use of these structures is to be able to demonstrate controllable quantum effects.

Figure 1 shows two dots contacted to source and drain electrodes. The material is a 30 nm thick layer of highly doped n-type $Si_{0.9}Ge_{0.1}$ grown on an undoped silicon-

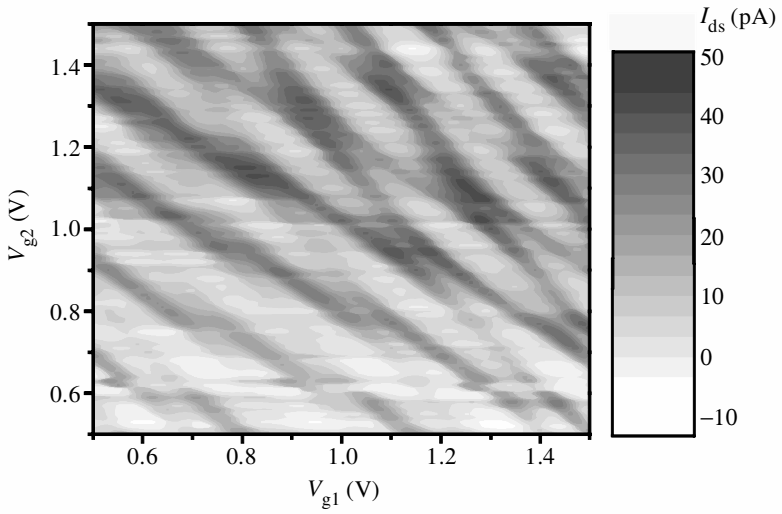

Figure 2. Measurement of current passing through the device as a function of the potentials on gates g1 and g2. The hexagonal pattern that the current maxima form shows that the dots are in an intermediate coupling regime, with the inter-dot conductance $G_{\mathrm{int}} = 0.8(2e^2/h)$. The disappearance of the hexagon sides at low V_{g1} and V_{g2} indicates that the device is becoming less strongly coupled to its leads.

on-insulator wafer. This device was fabricated by using EBL to pattern a PMMA resist layer, followed by lift-off of an evaporated aluminium layer. This patterned aluminium was then used as a sacrificial self-aligned mask for reactive ion etching of the doped SiGe layer. A high density of states at the semiconductor surface depletes the charge carriers by *ca.* 10 nm; hence the electronic size of the dots (*ca.* 20 nm) is significantly smaller than their diameter (*ca.* 40 nm). Because of this depletion, and the random distribution of dopants, the constrictions behave as tunnel barriers. The electrochemical potentials of the dots and the heights of the tunnel barriers can be controlled by varying the potential on the electrostatic gates g1, g2 and g3. In related devices made from a GaAs/AlGaAs two-dimensional electron gas, molecular states corresponding to the bonding and anti-bonding states of a diatomic molecule have been observed (Blick *et al.* 1998; Oosterkamp *et al.* 1998). This indicates a coherent coupling between the dots, which would potentially allow quantum logic to be performed.

In the SiGe double dots these states are still to be observed, but a large degree of control over the confinement potential and the electron number in the system has been shown. Figure 2 shows the results of an experiment where gates g1 and g2 are swept in potential. The device is measured at millikelvin temperatures in a dilution refrigerator and has a small bias applied (100 μV). The current passing through the device is measured and is represented by the grey scale. The hexagonal characteristic of the current maxima indicate that it is possible to independently control the number of electrons on each dot by changing the gate potentials (Adourian *et al.* 1996). Each time a maximum is crossed, an electron is added or removed from one of the dots. In other regions of the parameter space of the device double-dot–single-dot transitions have been observed. These show that the electrostatic gates can change the character of the system as well as the electron number.

Further studies need to be carried out in order to ascertain the presence of the molecular states and to test their controllability and decoherence time. However, the read-out technology (single-electron transistors) is relatively mature (Cain *et al.* 2002), and the fabrication method allows for integration of more devices. The compatibility with silicon processing offers a route to interfacing with an on-chip classical computer.

3. Epitaxial quantum dots

Quantum dots can form spontaneously during growth of semiconductor materials in the so-called Stranski–Krastanow mode. If you are growing a given crystal, such as GaAs, and you then switch the sources to grow a different composition that would naturally have a larger lattice constant, such as InGaAs, then, although initially there may be a wetting layer of the new composition, the growth quickly changes to three-dimensional islands to relax the mismatch strain. This phenomenon can be used to create layers of self-assembled QDs. Within a single layer the dots tend to have a random distribution of size and spacing, which makes them not very suitable for quantum computing. However, if a layer of dots is capped by further growth of the initial substrate material, and then a further layer of dots is grown, the strain field due to the first layer of dots promotes growth of dots directly above them. This process can be repeated to form extended stacks of QDs. With skill, the size of the dots within a stack can be made reasonably reproducible, and the spacing can be controlled to vary the interaction strength between dots. Stacked QDs can also be grown in the new nitride semiconductor materials. But before this can be exploited, it is first necessary to demonstrate that the lifetime and dephasing time of quantum states in the dots are sufficiently long when compared with typical logic gate operation time-scales.

There is quite a wide choice of ways in which quantum information can be embodied in stacked QDs (D'Amico *et al.* 2002). One possibility is in the form of charge distributions, in much the same way as in the nanofabricated structures described above, with the further possibility of controlling the interaction between them via the coherent control of excitons in the spacing layer (Heberle *et al.* 1996). Excitons can also be used to encode the information in the dots, either in the form of spin, which itself can be coherently controlled, or through the presence or absence of excitons in the dots (Lovett *et al.* 2003). If you allow up to two excitons in a single dot, then immediately you have a coupling scheme that allows a controlled-NOT (CNOT) gate, because the energy of the second exciton will be dependent on the presence of the first, but this scheme is not easy to scale up to many qubits. A CNOT gate can also be made by embodying qubits by the presence or absence of an exciton in each of two adjacent QDs. The coupling between two dots is illustrated schematically in figure 3. The dipole interaction between excitons in the dots can be modulated by applying an external electric field. Because of this interaction, the energy difference between $|00\rangle$ and $|01\rangle$—where the first digit refers to the first dot, and the second digit to the second dot, and '0' and '1' correspond to the absence and presence of an exciton, respectively—is different from the energy difference between $|10\rangle$ and $|11\rangle$. Thus, for example, a CNOT logic operation can be realized by applying a pulse of photon energy ε_{12} to the coupled-dot system (see figure 3). This will flip the state

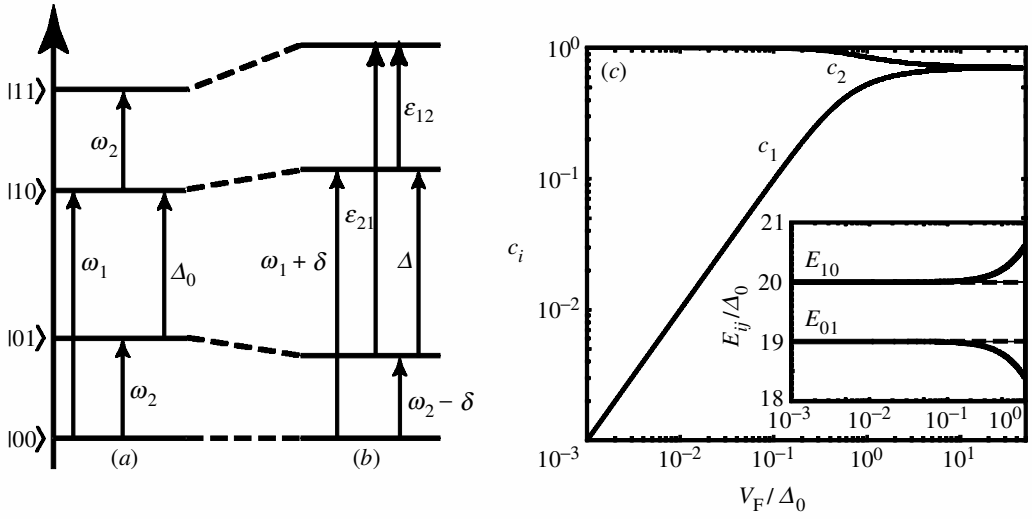

Figure 3. Energy levels in two QDs in (*a*) the absence and (*b*) the presence of the exciton–exciton Coulomb interaction V_{XX} and Förster coupling V_F for dots of different sizes. $\varepsilon_{12} = \omega_2 + V_{XX} - \delta$, $\varepsilon_{21} = \omega_1 + V_{XX} + \delta$, $\delta = V_F^2/\Delta_0$. $\Delta_0 \equiv \omega_1 - \omega_2$ is the difference between the exciton creation energy for dot I and that for dot II. (*c*) Main graph: computational basis-state mixing coefficients c_i as a function of V_F/Δ_0. Inset: eigenenergies E_{01} and E_{10} of plot (*b*) as a function of V_F/Δ_0 for $\omega_1/\Delta_0 = 20$.

of the second qubit if and only if the first qubit is in the state $|1\rangle$, i.e. if there is an exciton in the first dot.

Exciton lifetimes are generally quite short compared with electron charge or spin lifetimes; so a key question is whether they can ever be long enough to be useful. The lifetimes and dephasing times must be compared with the time required for an operation, which in experiments of this type is typically measured in femtoseconds. In InGaAs/GaAs QDs, exciton lifetimes can be as long as $T_1 = 900$ ps (Wang *et al.* 1994), with dephasing times $T_2 = 630$ ps (Borri *et al.* 2001). A series of measurements on GaN/AlN dots is shown in figures 4 and 5. The dots were grown by molecular beam epitaxy, and the structure is illustrated in the inset of figure 4. The dots were illuminated with a wavelength of 256 nm, and photoluminescence (PL) spectra were measured from room temperature to 4.2 K (see figure 4). The peak at 3.36 eV is strongly temperature dependent, decreasing as the temperature is raised. Time-correlated photon counting was used to measure the time dependence of the PL at 4.2 K following excitation (see figure 5). This peak exhibits a bi-exponential decay, in which we attribute the faster rate to the GaN wetting layer and the slower rate to the GaN/AlN dots.

Separate experiments, not shown here, have been performed on both InAs dot samples and GaInN dot samples that had been masked, so that only a few dots were illuminated and measured through a small aperture. These measurements reproducibly show sharp spectral lines, corresponding to excitation energies of states that are geometrically confined by the dots (Oliver *et al.* 2003). The measurements in figure 4 were taken from unmasked samples, and therefore include the spectra from a large number of dots. Because of the variation in dot size, the PL from the dots covers a broad range of wavelengths. Illustrative time-resolved PL curves are shown in

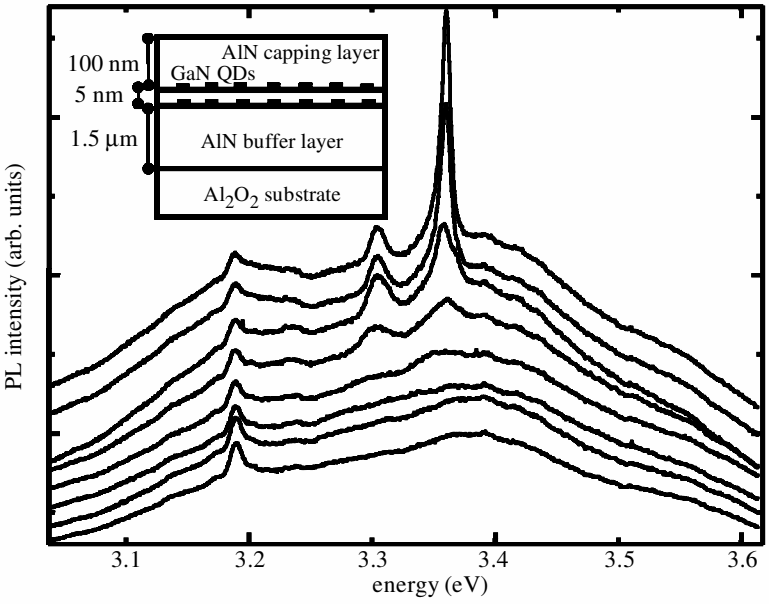

Figure 4. Time-resolved and time-integrated spectra of GaN QDs recorded with $\lambda_{ex} = 256$ nm. The PL spectra were recorded at 4.2 K, 18 K, 50 K, 100 K, 149 K, 200 K, 250 K and 285 K from the top line to the bottom one. A schematic of the fabricated GaN/AlN material studied is shown with the time-integrated PL spectra.

figure 5, with exciton decay times up to 5.7 ns. In $In_{0.6}Ga_{0.4}As/GaAs$ self-assembled QDs, the dephasing time can be almost as long as the relaxation time (Bayer & Forchel 2002). If the dephasing time of GaN/AlN dots similarly approaches the decay time, then this could be approximately 10^4 times a typical gate operation time. This ratio corresponds to the intrinsic characteristics of these exciton systems: techniques may become available to extend coherence times (e.g. via applying an electric fields to partly separate the electron and hole). Exciton systems constitute the fast end of the spectrum of proposals for quantum computing, with a clock cycle that may approach 1 THz. Although this is not the fundamental measure of merit for a quantum computer, it is nevertheless an attractive characteristic, and may be important for repeaters in quantum communication.

The dephasing time can be determined experimentally either from measurements of the line shape or from coherent control experiments. These experiments may be extended to individual dots using low dot densities and masking, and to the interactions between dots in a stack. It should also be possible to investigate the use of electric fields to address individual dots and to control the interaction between dots, and then to use coherent control for single-qubit and two-qubit manipulations. The theory is in place for the coupling between excitons in adjacent dots, vertical stacks of similar dots can be grown, and the individual exciton lifetime in nitride materials is demonstrated to be several nanoseconds.

4. Endohedral fullerenes in nanotubes

If there were a prize for the most versatile element in the periodic table, carbon would be likely to win it. The discovery of fullerene molecules of C_{60} and higher numbers of

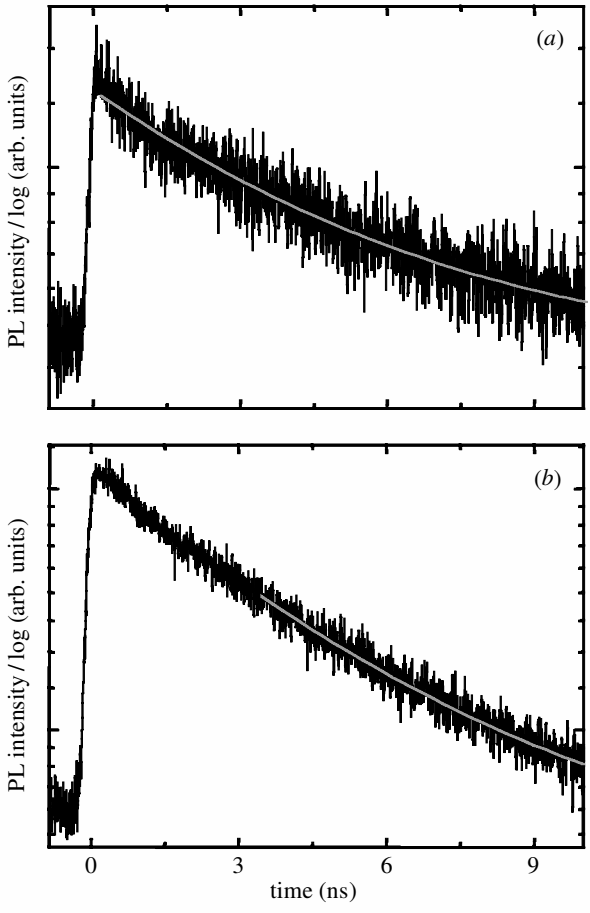

Figure 5. Single-photon counting traces of GaN QDs recorded at 4.2 K with $\lambda_{ex} = 256$ nm and monitored at (*a*) 3.25 eV ($\tau_1 = 5.7$ ns) and (*b*) 3.54 eV ($\tau_1 = 3.7$ ns).

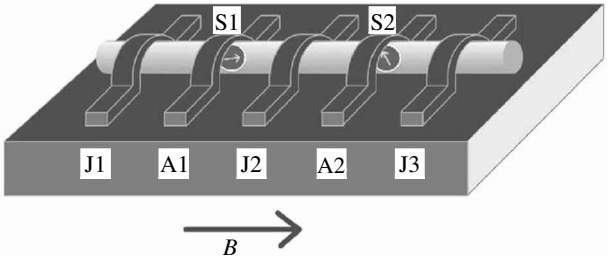

Figure 6. A scheme for an array of qubits in a nanotube. The 'A' electrodes are for addressing individual qubits, and the 'J' electrodes are for controlling the interactions between them.

carbon atoms (Kroto *et al.* 1985) was rapidly followed by the discovery of nanotubes (Iijima & Ichihashi 1993), which can be thought of as rolled-up sheets of graphene. It turns out to be possible to fill nanotubes with a wide range of materials (Sloan *et al.* 1998; Smith *et al.* 1998; Mittal *et al.* 2001) and this suggests the possibility of using nanotubes to create molecularly self-assembled arrays of structures suitable

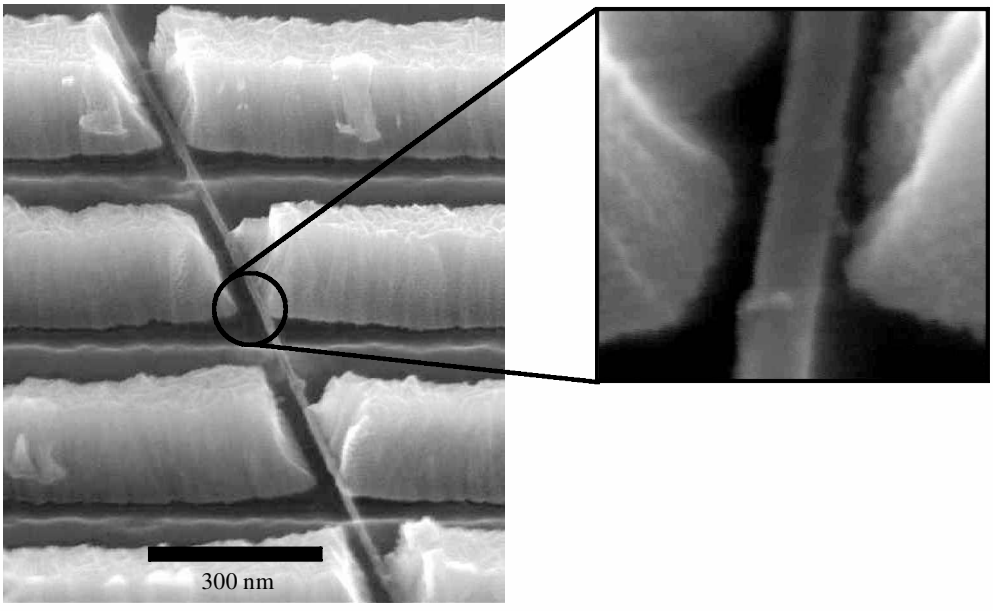

Figure 7. Self-aligned electrodes fabricated by evaporating 100 nm of chromium onto a multi-walled nanotube on a corrugated substrate.

for quantum computing. The conceptual principle of a proposed scheme is illustrated in figure 6. It consists of a single-walled carbon nanotube on an insulating substrate such as SiO_2. The nanotube contains discrete units (labelled S1 and S2) which can embody a qubit, here taken to be in the form of an electron spin. We describe the range of possible realizations for these units below. Individual qubits can be addressed by passing a current through electrodes labelled A1 and A2, which thus change the local magnetic field and hence the electron-spin resonance frequency. If the interaction between qubits is mediated through conduction electrons in the nanotube, then it can be modulated by applying potentials to electrodes J1, J2, J3. Thus the A and J gates together provide sufficient control to perform both one- and two-qubit gates, and hence universal computation. The structure could contain as many elements as you like, so that extended calculations could be performed. This conceptual scheme has a number of attractive features, but could it ever be made?

Several aspects of the physics required for such a nanotube quantum logic gate are now well established. Coherent transport of electrons in nanotubes has been demonstrated over distances of hundreds of nanometres in experiments with ferromagnetic contacts to the nanotubes, in which abrupt changes in resistance are observed that are associated with the magnetizations of the electrodes changing at slightly different magnetic fields (Tsukagoshi *et al*. 1999). Modulation of charge-carrier density in nanotubes has been demonstrated in several laboratories in the form of nanotube field effect transistors and classical logic elements (Tan *et al*. 1998; Yao *et al*. 1999; Rueckes *et al*. 2000). Figure 7 illustrates a new fabrication technique for self-aligned gate electrodes. Using EBL and wet etching, a ditch is created that passes under a section of the nanotube, so that it is suspended. Metal is then evaporated onto the sample. The metal grain structure grows vertically and, where the nanotube lies across the ditch, the metal settles on it like snow on a fence, separated from the

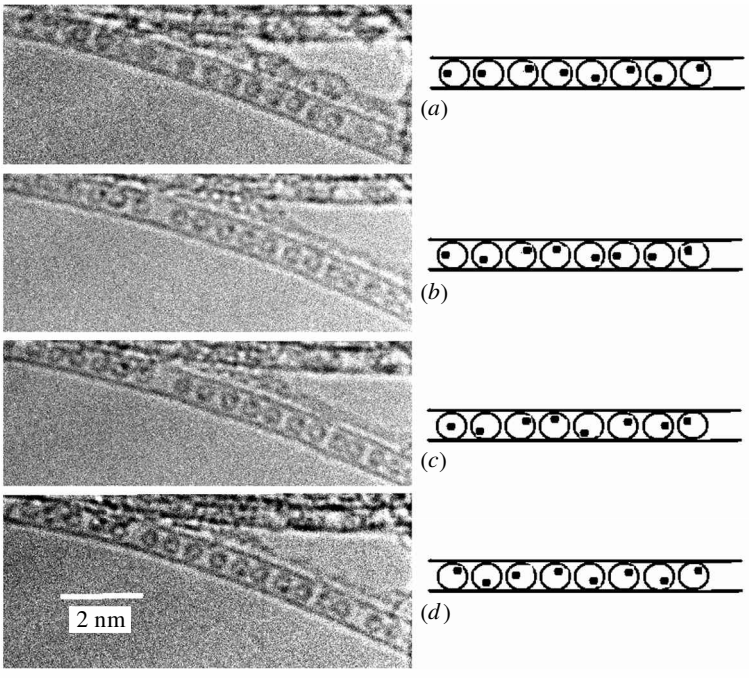

Figure 8. A series of successive HRTEM images of a single-walled nanotubes filled with $i\mathrm{CeC}_{82}$ fullerene (left) and their schematics (right). Images (*a*)–(*d*) were taken at 30 s time-intervals. Dark spots within fullerene cages correspond to individual atoms of Ce.

surrounding metal. A continuous electrode forms in the remainder of the ditch on each side of the nanotube. During the final lift-off process, the metal deposited on the nanotubes comes away, leaving electrodes very close to, but not touching, the nanotube.

Single-walled carbon nanotubes can be filled with a wide range of materials, and the structures can be imaged with high-resolution transmission electron microscopy (HRTEM) (Meyer *et al.* 2000). It is even possible to image the electronic interaction of the filling species with the walls of the nanotube using scanning tunnelling microscopy (Lee *et al.* 2002). Nanotubes can be filled with their older cousins, fullerene molecules, to make structures that look like pea pods (Kataura *et al.* 2001). It is possible to insert other atoms inside fullerene molecules, and in many cases these endohedral fullerenes have extremely sharp electron-spin resonance lines (Knapp *et al.* 1997; Seifert *et al.* 1998). They offer the possibility of embodying qubits in the different electron-spin states in an external magnetic field. Figure 8 shows a pea-pod structure of $i\mathrm{CeC}_{82}$ (sometimes written $\mathrm{Ce@C}_{82}$) in a single-walled nanotube. The cerium atoms can be seen inside the fullerene cages, which rotate in successive images under the influence of the electron beam.

The endohedral fullerene with the longest electron-spin resonance lifetime is $i\mathrm{NC}_{60}$ (Meyer *et al.* 2002; Shinohara 2000; Liu & Sun 2000). At room temperature, $T_1 = 120\,\mu\mathrm{s}$, $T_2 = 20\,\mu\mathrm{s}$; at 5 K the relaxation time is several seconds (Harneit 2002). Until recently the yield was very poor, so that it was available only in extremely low concentrations (Goedde *et al.* 2001). The reason it is difficult to purify is related to the reason why the spin lifetime is so long: the nitrogen sits in the centre of the

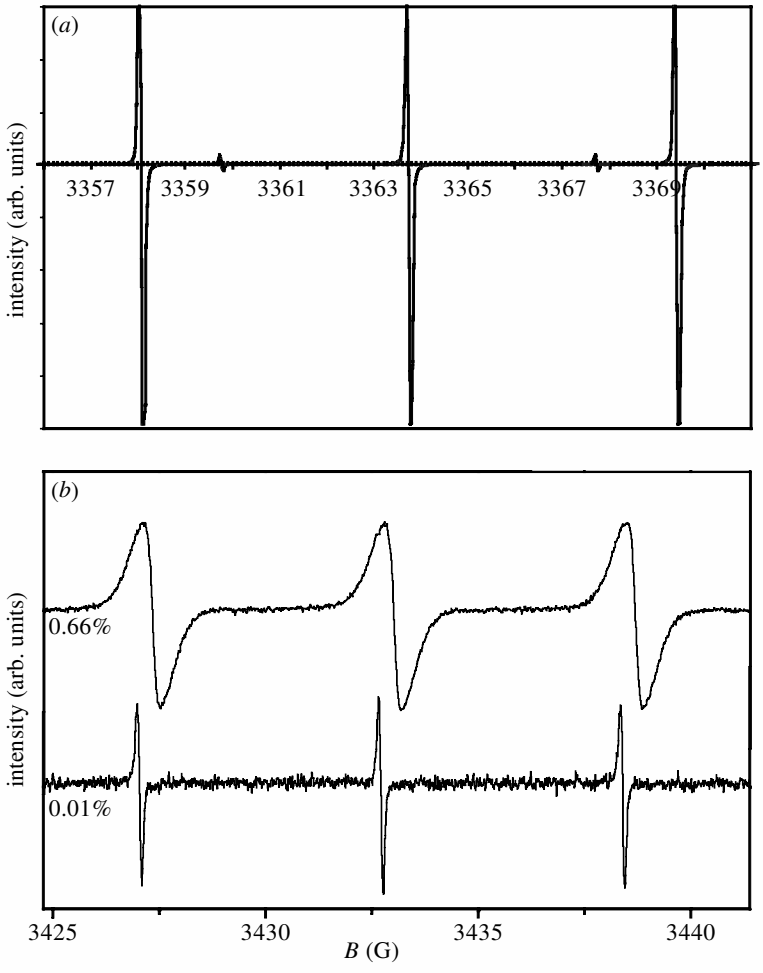

Figure 9. Electron-spin resonance spectrum of purified iNC$_{60}$ at X-band (*ca.* 9 GHz). (*a*) Pure iNC$_{60}$ in CS_2 solution, at room temperature. The three main peaks come from the hyperfine structure: ^{14}N has a nuclear spin $I = 1$; the two smaller peaks correspond to the ^{15}N isotope which has less than 0.5% natural abundance and $I = \frac{1}{2}$. (*b*) Powder samples of iNC$_{60}$ at room temperature with the approximate concentrations indicated.

cage and interacts only very weakly with it (Greer 2000; Park *et al*. 2002). By using recycling high-performance liquid chromatography, and using a very large number of cycles, it has eventually proved possible to achieve arbitrarily high concentrations, currently exceeding 95%. Figure 9 shows spectra from high purity samples. The spectrum from the liquid illustrates the narrow line width, which is less than 2 μT; the spectrum from the solid shows how the line is broadened by spin-spin interactions.

Many challenges remain for this kind of approach. The dephasing times of endohedral species in nanotubes need to be determined, and the nature of the interactions between them need to be understood and quantified. It may be necessary to control the spacing of the qubits. Read-out of a single-electron spin remains a common hurdle for any solid-state spin-based scheme. But great progress has been made in

fabricating the kinds of molecularly self-assembled structures that would be needed for the experiments that will begin to answer such questions.

5. Global addressing

All of the nanostructures described here are small. At most the separation of the qubits will be a few tens of nanometres, and in the molecularly self-assembled structures it is scarcely more than 1 nm. The eventual goal, when manipulation has been achieved with one and two qubits, will be to scale up successful implementations to more qubits. The problems associated with individually addressing a large number of such tiny elements so close together might seem intractable. But this may not be necessary.

Various schemes have been devised that allow quantum computing to be performed without local control of the interaction between qubits. If qubits can be made in two varieties, A and B, for example, in a one-dimensional array of the form ABABAB (though other configurations are also possible), then you need to be able to address all the 'A's separately from all the 'B's, but you do not need to address each A or each B individually (Benjamin 2000). You also need to be able to control and measure the qubits at each end of the array individually, for purposes of input and output. If the interaction between the qubits does not transfer energy, like the Ising interaction, then this is sufficient. If the interactions between qubits can transfer energy, like the Heisenberg interaction, then you also need to be able to control the interactions between A–B pairs separately from the interaction between B–A pairs (Benjamin 2002). Within these schemes, it is possible to pass quantum information along the array in one direction, and pass control information (the program) along the array in the other direction. The directions can be reversed as required. The user can choose whether to let qubits and program bits pass through each other transparently, or to let them interact so that the program bit acts as a control on what happens to the qubit. Sequences can be combined to form a set of one- and two-qubit gates that are universal for quantum computing.

Each of the candidate implementations described here would be amenable to this kind of architecture. The nanofabricated devices could be made in alternating sizes, or placed at alternating distances from global control electrodes. The stacked epitaxial QDs could have alternating sizes or compositions. The nanotubes could be filled with alternating endohedral fullerenes. This may prove to be a key insight for eventual scalability of nanoscale solid-state quantum computing.

The work described here is supported through the Foresight LINK Award *Nanoelectronics at the Quantum Edge*, funded by the DTI, EPSRC and Hitachi Europe Ltd. T.J.S.D. thanks The Royal Society for a Joint Research Project (Japan), the EPSRC for grant GR/R55313/01, and Queen Mary, University of London, for a College PhD Studentship to M.K. S.C.B. is supported by a University Research Fellowship from The Royal Society and B.W.L. thanks St Anne's College, Oxford, for a Junior Research Fellowship. The iNC$_{60}$ sample for purification was produced by M. Waiblinger and A. Weidinger, of the Hahn–Meitner Institute, Glienickerstraße 100, Berlin 14099, Germany.

References

Adourian, A. S., Livermore, C., Westervelt, R. M., Campman, K. L. & Gossard, A. C. 1996 Single electron charging in parallel coupled quantum dots. *Superlattices Microstruct.* **20**, 411–417.

Bayer, M. & Forchel, A. 2002 Temperature dependence of the exciton homogeneous linewidth in $In_{0.60}Ga_{0.40}As/GaAs$ self-assembled quantum dots. *Phys. Rev.* B **65**, 041308(R).

Benjamin, S. C. 2000 Schemes for parallel quantum computation without local control of qubits. *Phys. Rev.* A **61**, 020301.

Benjamin, S. C. 2002 Quantum computing without local control of qubit–qubit interactions. *Phys. Rev. Lett.* **88**, 017994.

Blick, R. H., Pfannkuche, D., Haug, R. J., von Klitzing, K. & Eberl, K. 1998 Formation of a coherent mode in a double quantum dot. *Phys. Rev. Lett.* **80**, 4032–4035.

Borri, P., Langbein, W., Schneider, S., Woggon, U., Sellin, R. L., Ougang, D. & Bimberg, D. 2001 Ultralong dephasing time in InGaAs quantum dots. *Phys. Rev. Lett.* **87**, 157401.

Cain, P. A., Ahmed, H. & Williams, D. A. 2002 Hole transport in coupled SiGe quantum dots for quantum computation. *J. Appl. Phys.* **92**, 346–350.

D'Amico, I., De Rinaldis, S., Zanardi, P. & Rossi, F. 2002 Quantum information/computation processing with self-assembled macroatoms. *Physica Status Solidi* B **233**, 377–384.

Goedde, B., Jakes, P., Waiblinger, M., Dinse, K. P. & Weidinger, A. 2001 Chromatographic separation of $N@C_{60}/C_{60}$ and $N@C_{70}/C_{70}$ mixtures. *Fullerene Sci. Technol.* **9**, 329–337.

Greer, J. C. 2000 The atomic nature of endohedrally encapsulated nitrogen $N@C_{60}$ studied by density functional and Hartree–Fock methods. *Chem. Phys. Lett.* **326**, 567–572.

Harneit, W. 2002 Fullerene-based electron-spin quantum computer. *Phys. Rev.* A **65**, 032322.

Heberle, A. P., Baumberg, J. J., Binder, E., Kuhn, T., Kohler, K. & Ploog, K. H. 1996 Coherent control of exciton density and spin. *IEEE J. Select. Topics Quant. Electron.* **2**, 769–775.

Iijima, S. & Ichihashi, S. 1993 Single-shell carbon nanotubes of 1 nm diameter. *Nature* **363**, 603–605.

Kataura, H., Maniwa, Y., Kodama, T., Kikuchi, K., Hirahara, K., Suenaga, K., Iijima, S., Suzuki, S., Achiba, Y. & Kratschmer, W. 2001 High-yield fullerene encapsulation in single-wall carbon nanotubes. *Synth. Met.* **121**, 1195–1196.

Knapp, C., Dinse, K. P., Pietzak, B., Waiblinger, M. & Weidinger, A. 1997 Fourier transform EPR study of $N@C_{60}$ in solution. *Chem. Phys. Lett.* **272**, 433–437.

Kroto, H. W., Heath, J. R., O'Brien, S. C., Curl, R. F. & Smally, R. E. 1985 C_{60}: Buckminsterfullerene. *Nature* **318**, 162–163.

Lee, J. (and 10 others) 2002 Bandgap modulation of carbon nanotubes by encapsulated metallofullerenes. *Nature* **415**, 1005–1008.

Liu, S. & Sun, S. 2000 Recent progress in the studies of endohedral metallofullerenes. *J. Organomet. Chem.* **599**, 74–86.

Lovett, B. W., Reina, J. H., Nazir, A., Kothari, B. & Briggs, G. A. D. 2003 Resonant transfer of excitons and quantum computation. (Preprint quant-ph/0209078.)

Meyer, R. R., Sloan, J., Dunin-Borkowski, R. E., Kirkland, A. I., Novotny, M. C., Bailey, S. R., Hutchison, J. L. & Green, M. L. H. 2000 Discrete atom imaging of one-dimensional crystals formed within single-walled carbon nanotubes. *Science* **289**, 1324–1326.

Meyer, C., Harneit, W., Lips, K. & Weidinger, A. 2002 Alignment of the endohedral fullerenes $N@C_{60}$ and $N@C_{70}$ in a liquid-crystal matrix. *Phys. Rev.* A **65**, 061201(R).

Mittal, J., Monthioux, M., Allouche, H. & Stephan, O. 2001 Room temperature filling of single-wall carbon nanotubes with chromium oxide in open air. *Chem. Phys. Lett.* **339**, 311–318.

Oliver, R. A., Briggs, G. A. D., Kappers, M. J., Humphreys, C. J., Rice, J. H., Smith, J. D. & Taylor, R. A. 2003 InGaN quantum dots grown by MOVPE employing a post-growth nitrogen anneal. *Appl. Phys. Lett.* (In the press.)

Oosterkamp, T. H., Fujisawa, T., van der Wiel, W. G., Ishibashi, K., Hijman, R. V., Tarucha, S. & Kouwenhoven, L. P. T. 1998 Microwave spectroscopy of a quantum-dot molecule. *Nature* **395**, 873–876.

Park, J. M., Tarakeshwar, P., Kim, K. S. & Clark, T. 2002 Nature of the interaction of paramagnetic atoms (A = ^{4}N, ^{4}P, ^{3}O, ^{3}S) with π systems and C_{60}: a theoretical investigation of A$\cdots C_6H_6$ and endohedral fullerenes N@C_{60}. *J. Chem. Phys.* **116**, 10 684–10 691.

Rueckes, T., Kim, K., Joselevich, E., Tseng, G. Y., Cheung, C. L. & Lieber, C. M. 2000 Carbon nanotube-based nonvolatile random access memory for molecular computing. *Science* **289**, 94–97.

Seifert, G., Bartl, A., Dunsch, L., Ayuela, A. & Rockenbauer, A. 1998 Electron spin resonance spectra: geometrical and electronic structure of endohedral fullerenes. *Appl. Phys.* A **66**, 265–271.

Shinohara, H. 2000 Endohedral metallofullerenes. *Rep. Prog. Phys.* **63**, 843–892.

Sloan, J., Hammer, J., Zwiefka-Sibley, M. & Green, M. L. H. 1998 The opening and filling of single-walled carbon nanotubes (SWTs). *Chem. Commun.*, pp. 347–348.

Smith, B. W., Monthioux, M. & Luzzi, D. E. 1998 Encapsulated C_{60} in carbon nanotubes. *Nature* **396**, 323–324.

Stone, N. J. & Ahmed, H. 1998 *Appl. Phys. Lett.* **73**, 2134–2136.

Tan, S. J., Verschueren, A. R. M. & Dekker, C. 1998 Room-temperature transistor based on a single carbon nanotube. *Nature* **393**, 49–52.

Tsukagoshi, K., Alphenaar, B. W. & Ago, H. 1999 Coherent transport of electron spin in a ferromagnetically contacted carbon nanotube. *Nature* **401**, 572–574.

Wang, G., Fafard, S., Leonard, D., Bowers, J. E., Merz, J. M. & Petroff, P. M. 1994 Time-resolved optical characterization of InGaAs/GaAs quantum dots. *Appl. Phys. Lett.* **64**, 2815–2817.

Yao, Z., Postma, H. W. Ch., Balents, L. & Dekker, C. 1999 Carbon nanotube intermolecular junctions. *Nature* **402**, 273–276.

Yasin, S., Hasko, D. G. & Ahmed, H. 2001 Fabrication of < 5 nm width lines in poly(methyl methacrylate) resist using a water:isopropyl alcohol developer and ultrasonically-assisted development. *Appl. Phys. Lett.* **78**, 2760–2762.